tibody at a dilution of 1:1,000 (Y011052; Applied Biological Materials, Richmond, BC, Canada). This antibody was produced against a synthesized phosphopeptide spanning R-P-SP-Y-R, derived from the human CREB1 amino acid sequences surrounding the serine 133 residue (Ser-133), and purified by affinity-chromatography with an epitope-specific phosphopeptide. The specificity of the antibody was verified by western blot analysis of a human neuronal cell line exposed to forskolin in culture (not shown). After several washes, the tissue sections were incubated with horseradish peroxidase (HRP)-conjugated anti-rabbit antibody (Nichirei, Tokyo, Japan), and colorized with DAB substrate (Vector Laboratories, Burlingame, CA, USA), followed by a counterstain with hematoxylin. The adjacent sections were immunolabeled with mouse monoclonal anti-GFAP antibody (Nichirei). For negative controls, the step of incubation with primary antibodies was omitted.

3. Results

3.1. *Transcriptome dataset of Alzheimer disease hippocampus*

The dataset of Blalock et al. [10] contains genome-wide transcriptome of the hippocampus CA1 region, derived from nine control subjects, seven patients with incipient AD (IAD), eight with moderate AD, and seven with severe AD. They identified 3,413 all stages of AD-related genes (ADGs) and 609 IAD-related genes (IADGs) based on significant clinical and pathological correlations. We performed extensive curation of their data, and extracted 2,883 Entrez Gene IDs of ADGs, composed of 1,675 upregulated and 1,208 downregulated genes in all stages of AD patients versus control subjects (Supplementary Tables 1 and 2 online). We also identified 559 Entrez Gene IDs of IADGs, composed of 395 upregulated and 164 downregulated genes in IAD patients versus control subjects (Supplementary Tables 3 and 4 online).

3.2. *The molecular network analysis of ADGs and IADGs identified CREB as a central transcription factor*

First, we imported 2,883 Entrez Gene IDs of ADGs, along with the expression levels, into KeyMolnet (the version 4.9.9.616 of July 1, 2009). The common upstream search of the core contents generated a complex network composed of 508 fundamental nodes with 735 molecular relations, arranged with respect to subcellular location of the molecules by the editing function of KeyMolnet (Fig. 1). By statistical evaluation, the extracted network showed the most significant relationship with transcriptional regulation by CREB with the score of 229 and score (p) = 1.141E-069, where CREB is located as a common upstream transcription factor that has direct connections with 50 nodes, all of which are known CRE-responsive genes (Fig. 2 and Table 1). Unexpectedly, the CREB-regulated transcriptional network is comprised of not only 17 upregulated ADGs but also 26 downregulated ADGs. These results suggest not simply either overactivation or hypoactivation of CREB but an involvement of generalized deregulation of the CREB signaling pathway in the pathophysiology of AD. The second rank pathway was transcriptional regulation by nuclear factor kappa B (NF-κB) with the score of 158 and score (p) = 1.945E-048 (Supplementary Fig. 1 online), while the third rank was transcriptional regulation by vitamin D receptor (VDR) with the score of 140 and score (p) = 5.841E-042 (Supplementary Fig. 2 online).

Next, we imported 559 Entrez Gene IDs of IADGs and the expression levels into KeyMolnet. Subsequently, the common upstream search of the core contents generated a less complex network composed of 143 fundamental nodes with 190 molecular relations (Fig. 3). By statistical evaluation, the extracted network showed again the most significant relationship with transcriptional regulation by CREB with the score of 71 and score (p) = 3.325E-022, comprised of 5 upregulated and 5 downregulated IADGs (Fig. 4 and Table 1). These results suggest that functional impairment of CREB in the AD hippocampus is beginning at the early stage of the disease. The second rank pathway was transcriptional regulation by NF-κB or by glucocorticoid receptor (GR) with the identical score of 53 and score (p) = 1.163E-016 between both.

3.3. *Granulovacuolar degeneration in hippocampal neurons of AD brains expressed pCREB immunoreactivity*

It is well known that a wide range of extracellular stimuli activates CREB by inducing phosphorylation of Ser-133 on CREB, thereby it functions as a transcriptional activator [18,19]. Because the molecular network of both ADGs and IADGs reflects persistent impairment of CREB function in the AD hippocampus, we studied the expression of Ser-133-phosphorylated

Table 1
The list of 51 genes constructing the CREB-regulated transcriptional network in AD hippocampus

KeyMolnet symbol	Gene name	Upregulation or downregulation[a]	Involvement in IAD network	Swiss-Prot ID
14-3-3epsilon	14-3-3 protein epsilon	down		P62258
AChE	acetylcholinestrase	down		P22303
AhR	arylhydrocarbon receptor	km		P35869
BCKDH	branched-chain alpha-keto acid dehydrogenase	down		P09622, P11182, P12694, P21953
Bcl-2	B-cell lymphoma 2	up		P10415
BiP	78 kDa glucose-regulated protein	down	yes	P11021
BRCA1	breast cancer type 1 susceptibility protein	up		P38398
C/EBPb	CCAAT/enhancer binding protein beta	km	yes	P17676
CCK	cholecystokinin	down		P06307
CDK5	cyclin dependent kinase 5	down		Q00535
ChromograninA	chromogranin A	down		P10645
CPT	carnitine palmitoyl transferase	up	yes	P50416, Q92523, Q8TCG5, P23786
CREB	cAMP-response-element-binding-protein	km	yes	P16220
CRF	corticotropin-releasing factor	down	yes	P06850
cyclinA	cyclin A	down		P78396, P20248
cyto-c	cytochrome c	down		P99999
DIO2	type II iodothyronine deiodinase	down		Q92813
Egr1	early growth response protein 1	up		P18146
ENO2	neuron-specific enolase	down		P09104
FN1	fibronectin 1	down		P02751
GADD34	protein phosphatase 1, regulatory subunit 15A	up		O75807
GluR1	glutamate receptor 1	down		P42261
GR	glucocorticoid receptor	km	yes	P04150
GS	glutamine synthetase	down	yes	P15104
HO-1	heme oxygenase 1	up		P09601
ICAM-1	intercellular adhesion molecule 1	up		P05362
IGF1	insulin-like growth factor 1	down		P01343, P05019
IL-6	interleukin-6	up		P05231
JunD	transcription factor Jun-D	up	yes	P17535
LDH	L-lactate dehydrogenase	down		Q6ZMR3, Q9BYZ2, P00338, P07195, P07864
MITF	microphthalmia-associated transcription factor	up	yes	O75030
MnSOD	manganese superoxide dismutase	up		P04179
NF-L	neurofilament triplet L protein	down		P07196
NPY	neuropeptide Y	down		P01303
NR4A2	orphan nuclear receptor NR4A2	km		P43354
ODC	ornithine decarboxylase	up		P11926
PC	prohormone convertase	down		P29120, P16519, Q16549
PCB	pyruvate carboxylase	up	yes	P11498
PCNA	proliferating cell nuclear antigen	down		P12004
PER1	period circadian protein 1	up	yes	O15534
PER2	period circadian protein 2	up		O15055
Pit-1	pituitary-specific positive transcription factor 1	km	yes	P28069
PPT-A	preprotachykinin A	down	yes	P20366
proenkeph	proenkephalin	down		P01213, P01210
SGK	serum- and glucocorticoid-inducible kinase	up	yes	O00141, Q9HBY8, Q96BR1
SST	somatostatin	down	yes	P61278
STAT3	signal transducer and activator of transcription 3	km	yes	P40763
SynapsinI	synapsin-1	down		P17600
TGFb2	transforming growth factor beta 2	up		P61812
TyrAT	tyrosine aminotransferase	up		P17735
VIP	vasoactive intestinal peptide	down		P01282

Km represents additional nodes unlisted in the original set of 2,883 ADGs but automatically incorporated from KeyMolnet core contents following the network-searching algorithm.

CREB (pCREB) in 11 AD and 13 age-matched control brains by immunohistochemistry. The granular components of granulovacuolar degeneration (GVD), accumulated in the cytoplasm of hippocampal pyramidal neurons in both AD and non-AD brains, expressed strong immunoreactivity against pCREB (Fig. 5, panels a-d). However, the nuclei of hippocampal pyramidal neurons were devoid of pCREB immunoreac-

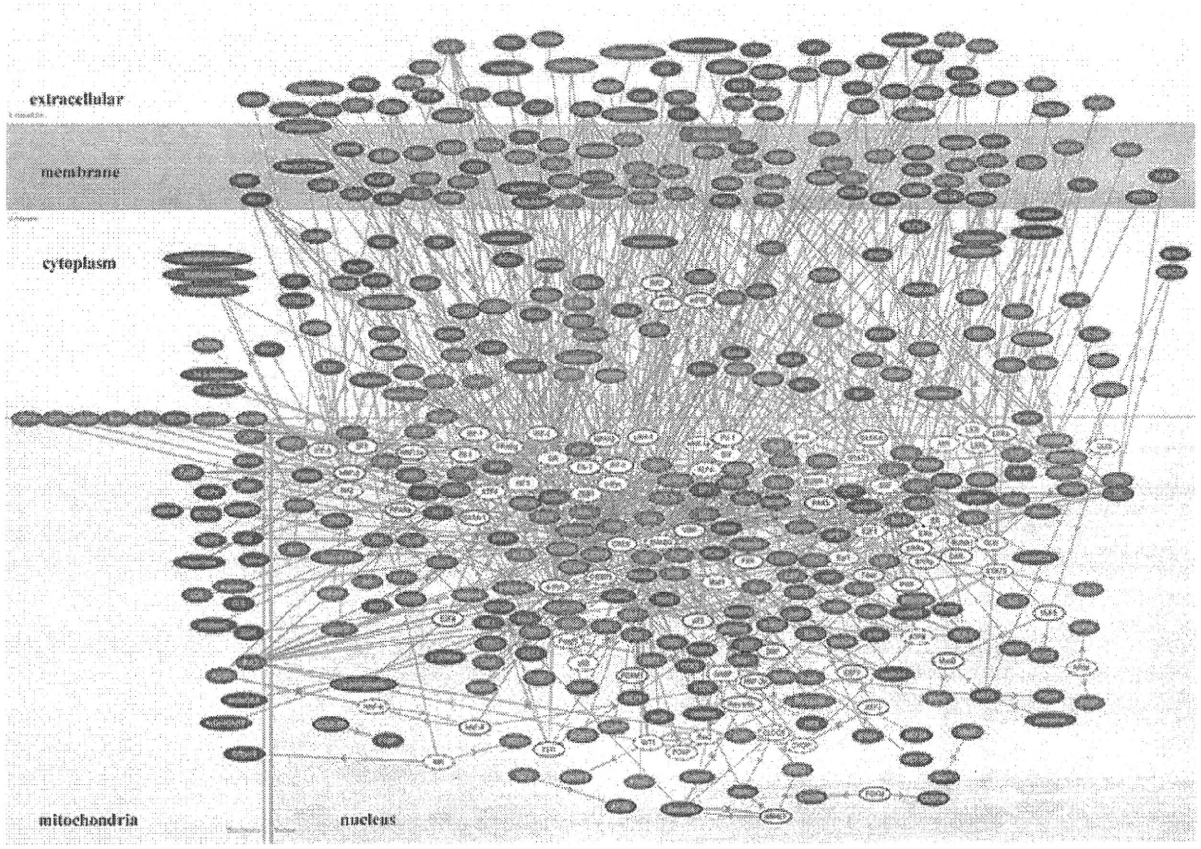

Fig. 1. Molecular network of all stages of AD-related genes (ADGs). The list of 2,883 Entrez Gene IDs corresponding to ADGs was imported into KeyMolnet. The common upstream search of the core contents generated a network composed of 508 fundamental nodes with 735 molecular relations, arranged with respect to subcellular location of the molecules. Red nodes represent upregulated genes, whereas blue nodes represent downregulated genes. White nodes exhibit additional nodes extracted automatically from the core contents incorporated in the network to establish molecular connections. The direction of molecular relation is indicated by red-colored dash line with arrow (transcriptional activation) or blue-colored dash line with arrow and stop (transcriptional repression).

tivity. In addition, the vacuolar component of GVD lacked pCREB immunoreactivity, while neuritic processes of hippocampal neurons expressed variable levels of pCREB immunoreactivity (Fig. 5, panel c). pCREB-immunoreactive GVD-bearing neurons were distributed chiefly in the CA1-CA3 sectors. Senile plaques and neurofibrillary tangles were completely devoid of pCREB immunolabeling. Although the number of pCREB-immunoreactive GVD-bearing neurons was varied among the cases, it was significantly greater in the hippocampus of AD compared with non-AD ($p = 0.00020$ by Mann-Whiteney's U test) (Fig. 6). pCREB-immunoreactive GVD-bearing neurons were occasionally found in the CA4 and subicular regions of AD brains, but barely detectable in the corresponding regions of non-AD brains. In both AD and non-AD brains, substantial numbers of neuronal axons distributed in the white matter of the motor cortex expressed intense pCREB immunoreactivity (Fig. 5, panel e). In both AD and non-AD brains, a subpopulation of reactive astrocytes and almost all ependymal cells expressed strong pCREB immunoreactivity, but it was located predominantly in their nuclei (Fig. 5, panel f). In both AD and non-AD brains, most neurons except for hippocampal pyramidal neurons did not express discernible pCREB immunoreactivity in their cell bodies and nuclei. Neither oligodendrocytes nor microglia expressed pCREB immunoreactivity in any cases examined.

4. Discussion

Since microarray analysis usually produces a large amount of gene expression data at one time, it is often difficult to find out the meaningful relationship be-

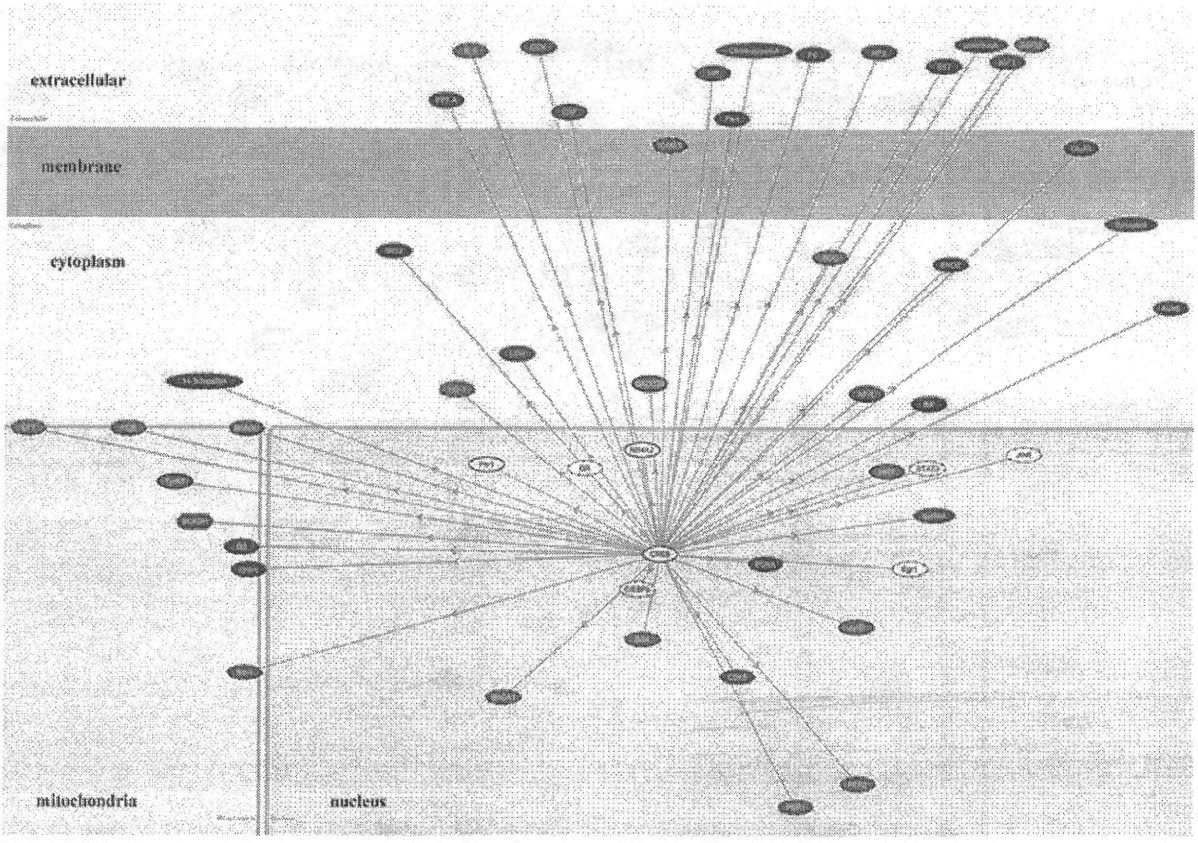

Fig. 2. The CREB-regulated transcriptional network of ADGs. The CREB-regulated transcriptional network extracted from the ADG network of Fig. 1 consists of a central node of CREB and 50 connecting nodes of CREB target genes listed in Table 1.

tween gene expression profile and biological implications from such a large quantity of available data. To overcome this difficulty, we have made a breakthrough to identify the molecular network most closely associated with microarray data by using a novel bioinformatics tool named KeyMolnet [12]. KeyMolnet includes the highly reliable information on a wide range of human proteins, small molecules, molecular relations, diseases, and drugs. All the contents are manually collected and carefully curated by experts from the literature and public databases. The application of KeyMolnet has an advantage that the user can easily merge microarray data with the comprehensive knowledgebase to characterize pathophysiologically meaningful networks from the high-throughput gene expression data [20,21]. In particular, the common upstream search is the most powerful approach to identify a battery of common transcription factors governing molecular networks closely associated with aberrant gene expression. By using KeyMolnet, we characterized the molecular network of 2,883 ADGs and 559 IADGs that show significant correlations with MMSE score and NFT burden in either all stages of AD or the early stage of AD [10]. We identified CREB as the central transcription factor that exhibits the most significant relevance to molecular networks of both ADGs and IADGs.

CREB is the prototype stimulus-inducible transcription factor binding as a dimer to a conserved cAMP-responsive element (CRE) of the target genes [18,19]. CREB is promptly activated in response to a wide range of extracellular stimuli, such as growth factors, peptide hormones, and neuronal activity, all of which activate various protein kinases such as PKA, mitogen-activated protein kinases (MAPKs), and Ca^{2+}/calmodulin-dependent protein kinases (CAMKs). They phosphorylate Ser-133 located in the KID domain of CREB. The phosphorylation of Ser-133 on CREB (pCREB) induces the recruitment of a transcriptional coactivator named CREB binding protein (CBP), thereby activates the expression of CRE-responsive genes. The CREB target genes play key roles in neuronal devel-

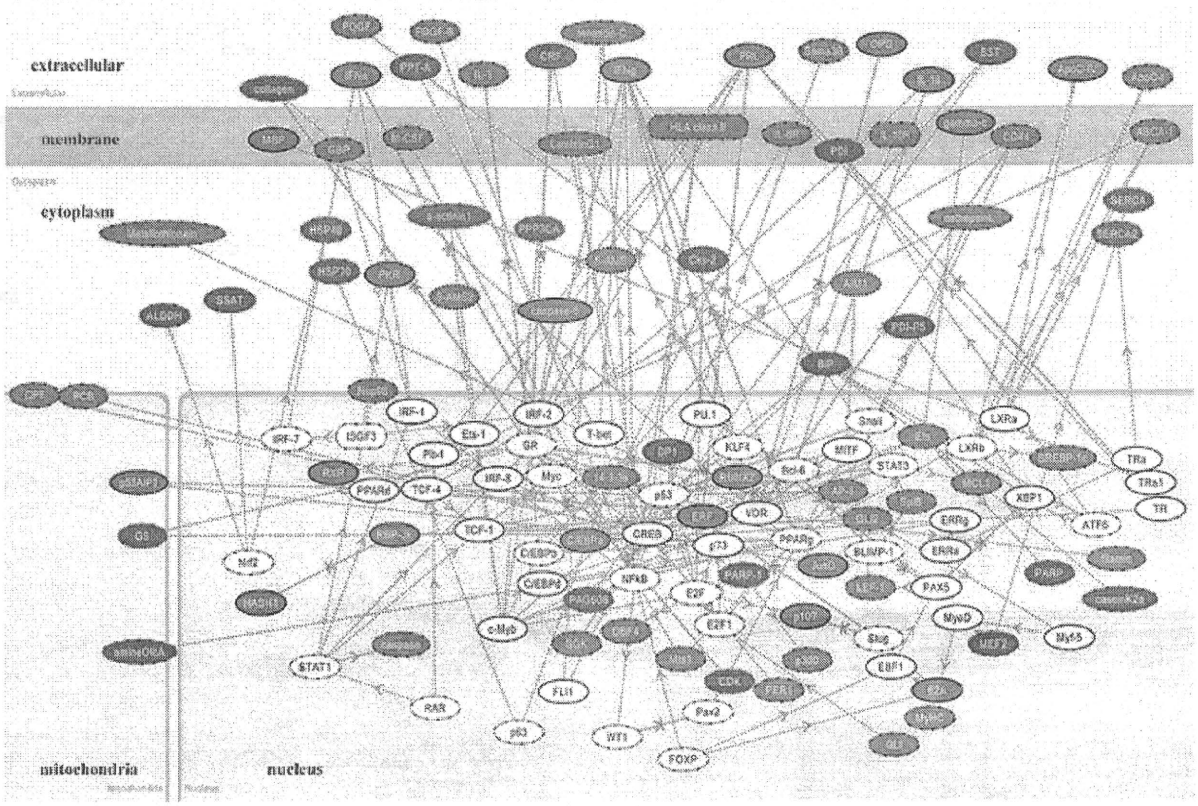

Fig. 3. Molecular network of incipient AD-related genes (IADGs). The list of 559 Entrez Gene IDs corresponding to IADGs was imported into KeyMolnet. The common upstream search of the core contents generated a network composed of 143 fundamental nodes with 190 molecular relations, arranged with respect to subcellular location of the molecules. Red nodes represent upregulated genes, whereas blue nodes represent downregulated genes. White nodes exhibit additional nodes extracted automatically from the core contents incorporated in the network to establish molecular connections. The direction of molecular relation is indicated by red-colored dash line with arrow (transcriptional activation) or blue-colored dash line with arrow and stop (transcriptional repression).

opment, synaptic plasticity, and neuroprotection in the central nervous system (CNS). Currently, we are able to search thousands of CREB target genes via the web-accessible database (natural.salk.edu/CREB) [22]. In the present study, the CREB-regulated transcriptional network consisted of both upregulated and downregulated sets of ADGs and IADGs. These observations suggest not simply either overactivation or hypoactivation of CREB but an involvement of generalized deregulation of the CREB signaling pathway in the pathophysiology of AD, emerging at the early stage of the disease.

To verify the *in silico* observations *in vivo*, we conducted immunohistochemical studies of 11 AD and 13 age-matched non-AD control brains by using anti-pCREB antibody. We identified aberrant pCREB immunoreactivity concentrated in granules of GVD in the hippocampus of both AD and non-AD brains, where the number of pCREB-immunoreactive GVD-bearing neurons was significantly greater in AD than non-AD cases. These results suggest that pCREB-immunoreactive GVD does not itself serve as an AD-specific diagnostic marker. However, these observations would support the hypothesis that sequestration of pCREB in GVD granules might be in part attributable to disturbed CREB-regulated gene expression in AD hippocampus.

Physiologically, CREB plays a pivotal role in the long-term memory formation in CA1 hippocampal neurons [23]. A previous study by western blot analysis showed that pCREB levels are reduced in AD brain tissues, although the cellular and subcellular location of pCREB was not characterized [24]. In a rat model, cortical impact injury induces a cognitive impairment, associated with reduced expression of CREB and target genes in the ipsilateral hippocampus [25]. A phosphodiesterase-4 inhibitor rolipram, by activating the cAMP/PKA/CREB signaling pathway, ameliorates deficits in long-term potential and cognitive function

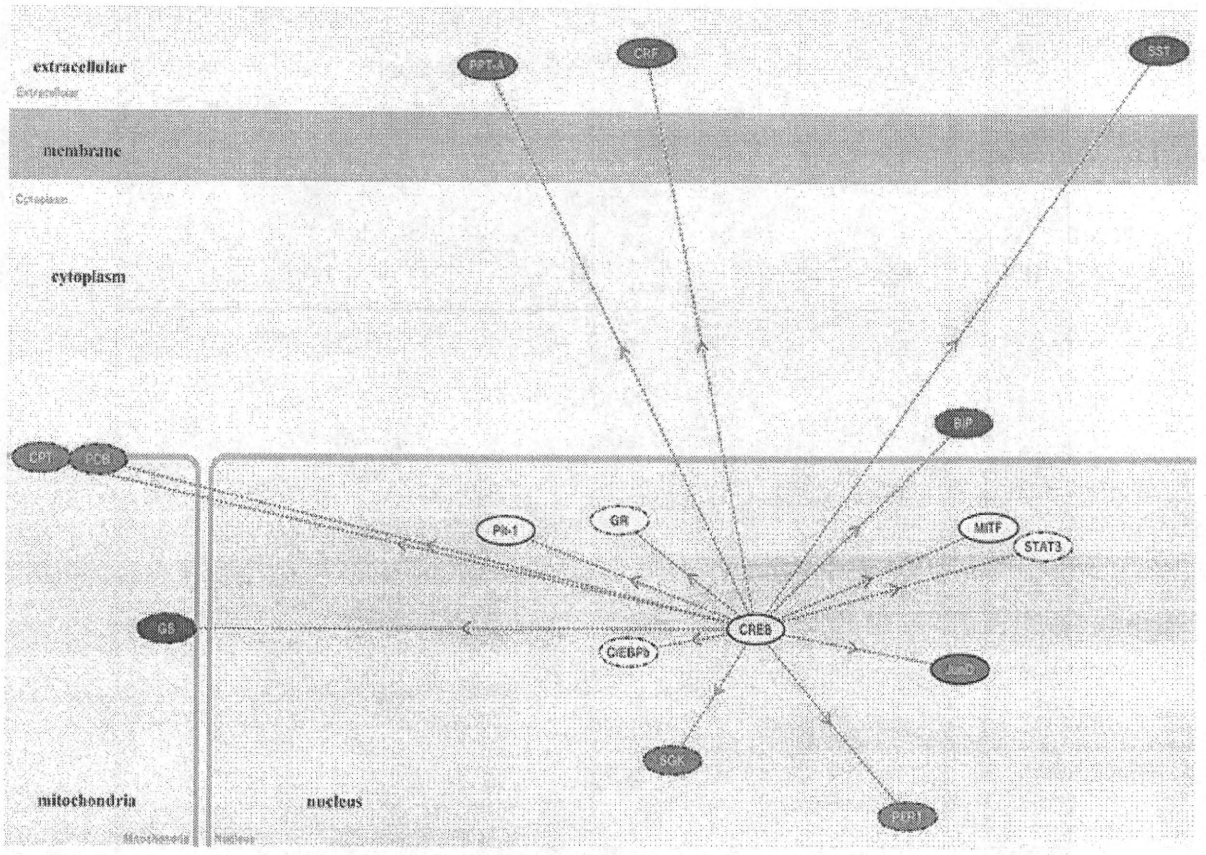

Fig. 4. The CREB-regulated transcriptional network of IADGs. The CREB-regulated transcriptional network extracted from the IADG network of Fig. 3 consists of a central node of CREB and 15 connecting nodes of CREB target genes listed in Table 1.

in a transgenic mouse model of AD [26]. Overactivation of calpain induces proteolysis of PKA subunits, resulting in inactivation of CREB in AD brains [27]. High levels of intracellular Aβ induce sustained hyperphosphorylation of CREB that blocks nuclear translocation of pCREB, resulting in inactivation of CREB-regulated gene expression [28]. The Aβ oligomers inactivate MAPKs, PKA, and cyclic GMP-dependent protein kinase essential for CREB activation in hippocampal neurons [29–31]. Long-term treatment with green tea catechin reduces the levels of Aβ oligomers, thereby restores the expression of CREB target genes, such as BDNF and PSD95, in the hippocampus [32]. All of these observations support a possible scenario that a defect in the CREB-mediated signaling pathway in hippocampal neurons causes cognitive disturbance during progression of AD. Therefore, CREB serves as a promising molecular target for treatment of dementia in AD [33].

The accumulation of misfolded cellular proteins within neurons, due to a defect in the clearance system, such as the ubiquitin-proteasome system (UPS) and the autophagic-lysosomal system, is a pathological hallmark of various neurodegenerative diseases [34]. Degradation of CREB involves nuclear export of CREB, modification by polyubiquitination, and processing for proteasomes, suggesting that UPS is a major system for CREB degradation under normal physiological conditions [35,36]. We identified an abnormal accumulation of pCREB in GVD granules of hippocampal neurons in AD brains. GVD is a pathological change characterized by electron-dense granules within double membrane-bound cytoplasmic vacuoles that highly resemble autophagosomes [37]. The emergence of GVD is confined to hippocampal pyramidal neurons of AD brains, and infrequently found in those of other neurodegenerative diseases. GVD is barely detectable in other brain regions. It plays a role in sequestration and degradation of unnecessary proteins and organelles in neurons exposed to aging-related stressful insults [37]. The active forms of caspase-3, glycogen synthase kinase-3β (GSK-3β), c-Jun N-terminal kinase

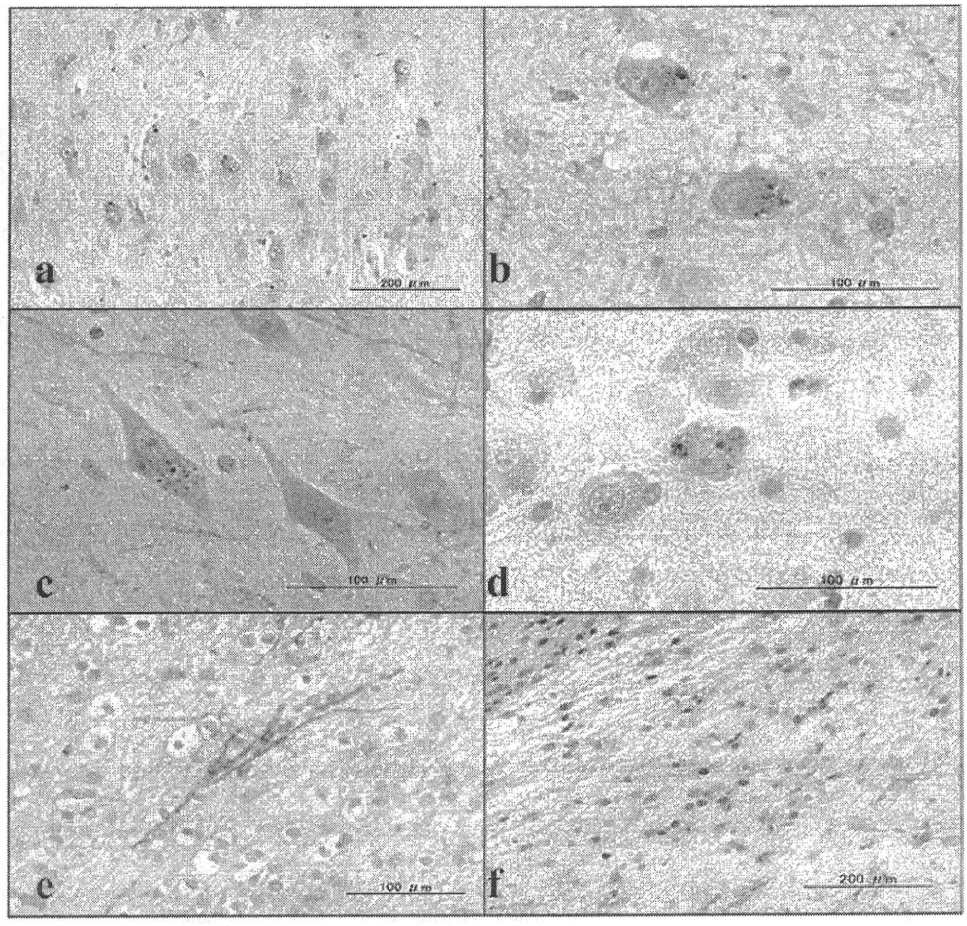

Fig. 5. pCREB immunoreactivity in AD and non-AD brains. The tissue sections of the hippocampus (HC) and the motor cortex (MC) of 11 AD patients and 13 other neurological disease (non-AD) patients were immunolabeled with an antibody against Ser-133-phosphorylated CREB (pCREB). (a) HC CA1 of a 59-year-old AD patient. The granular components of granulovacuolar degeneration (GVD) accumulated in the cytoplasm of pyramidal neurons exhibit strong pCREB immunoreactivity. (b) HC CA1 of a 68-year-old AD patient. The granular components of GVD accumulated in the cytoplasm of pyramidal neurons exhibit strong pCREB immunoreactivity. (c) HC CA3 of a 77 year-old AD patient. The vacuolar components of GVD are devoid of pCREB immunoreactivity. Neuritic processes of hippocampal neurons express variable levels of pCREB immunoreactivity. (d) HC CA1 of a 68 year-old myotonic dystrophy patient. The granular components of GVD accumulated in the cytoplasm of pyramidal neurons exhibit strong pCREB immunoreactivity. (e) MC of a 72-year-old AD patient. Substantial numbers of neuronal axons in the white matter of the motor cortex express strong pCREB immunoreactivity. (f) The periventricular white matter in the hippocampus of an 80 year-old AD patient. A subpopulation of reactive astrocytes express strong pCREB immunoreactivity located predominantly in their nuclei.

(JNK), c-Jun, pancreatic eIF2-alpha kinase (PERK), and TAR DNA-binding protein-43 (TDP-43), all of which are modified by phosphorylation, are found to be accumulated in GVD granules of hippocampal neurons in AD brains [38–43]. GVD granules also include cytoskeletal proteins, such as neurofilament, tubulin, and tau, along with ubiquitin [44,45]. At present, the precise implication of pCREB accumulation in GVD granules of hippocampal neurons in AD brains remains unknown. Importantly, degenerating neurons but not apparently healthy neurons in AD brains exhibit the profuse accumulation of autophagic vacuoles (AVs), owing to decreased clearance of AVs [46], suggesting an involvement of impaired autophagy function in formation of pCREB-accumulated GVD granules.

We found that neuronal axons, neuritic processes, and a subpopulation of reactive astrocytes also express pCREB immunoreactivity in both AD and non-AD brains. In a rat model of neuronal injury, reactive astrocytes express pCREB following intracerebroventricular injection of kinate [47]. In developing mouse DRG neurons, CREB protein is translated in response to NGF from the corresponding mRNA located in axons, and subsequently translocated to the cell body via a retro-

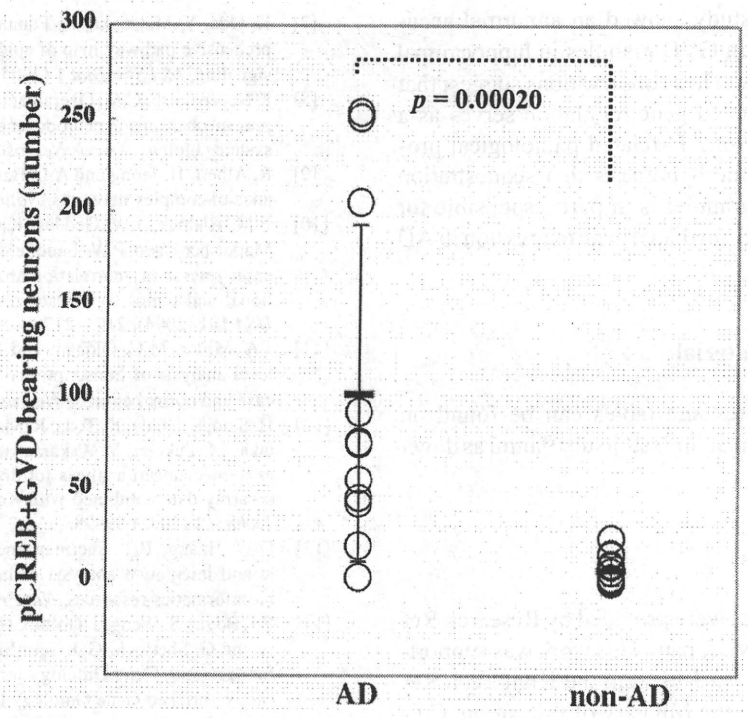

Fig. 6. The number of pCREB-immunoreactive GVD-bearing neurons in the hippocampus of AD and non-AD brains. The number of pCREB-immunoreactive GVD-bearing neurons was counted in the CA1, CA2, CA3 and CA4 sectors and the subiculum of the hippocampus, derived from 11 AD cases and 13 age and sex-matched other neurological disease (non-AD) cases. Non-AD cases include three patients with Parkinson disease (PD), two with multiple system atrophy (MSA), four with amyotrophic lateral sclerosis (ALS), and four with myotonic dystrophy. The total number in each case is plotted. The statistical difference in the numbers between AD and non-AD was evaluated by Mann-Whitney's U test.

grade axonal transport [48]. These observations would provide an explanation for glial or axonal location of CREB and pCREB.

We identified NF-κB-regulated gene expression as the second significant pathway in the molecular network of AGDs and IADGs (Supplementary Fig. 1 online). The NF-κB family, consisting of NF-κB1 (p50/p105), NF-κB2 (p52/p100), RelA (p65), RelB, and c-Rel, acts as a central regulator of innate and adaptive immune responses, cell proliferation, and apoptosis [49]. Under unstimulated conditions, NF-κB is sequestrated in the cytoplasm via non-covalent interaction with the inhibitor of NF-κB (IκB). Proinflammatory cytokines and stress-inducing agents activate specific IκB kinases that phosphorylate IκB proteins. Phosphorylated IκBs are ubiquitinated, and then processed for proteasome-mediated degradation, resulting in nuclear translocation of NF-κB that regulates the expression of hundreds of target genes by binding to the consensus sequence located in the promoter. Importantly, the expression of NF-κB p65 is enhanced in neurons, NFTs, and dystrophic neurites in the hippocampus and entorhinal cortex of AD brains [50]. A NF-κB-inducible microRNA, MiR-146a, reduces the expression of complement factor H (CFH), a negative regulator of proinflammatory responses in AD brains [51].

We also identified gene expression regulated by vitamin D receptor (VDR) as the third significant pathway in the molecular network of AGDs (Supplementary Fig. 2 online). Vitamin D plays a neuroprotective role by modulating neuronal calcium homeostasis. By forming a heterodimer with the retinoid X receptor (RXR), VDR activates the transcription of target genes with the vitamin D response element (VDRE) in the promoter. A significant association is found between VDR gene polymorphism and development of AD [52]. In AD brains, the expression of VDR and its target calbindin D28K is downregulated in hippocampal CA1 neurons [53].

In conclusion, KeyMolnet has effectively characterized molecular network of 2,883 ADGs and 559 IADGs. The common upstream search identified CREB as the principal transcription factor that regulates molecular networks of both ADGs and IADGs. Im-

munohistochemical study showed an abnormal accumulation of pCREB in GVD granules in hippocampal neurons of AD brains. These observations suggest that aberrant CREB-mediated gene regulation serves as a molecular biomarker of AD-related pathological processes, and support the hypothesis that sequestration of pCREB in GVD granules is in part responsible for deregulation of CREB-mediated gene expression in AD hippocampus.

5. Supplemental Material

Supplemental figures and tables can be found on http://www.my-pharm.ac.jp/~satoj/sub19.html as downloadable PDF files.

Acknowledegements

Human brain tissues were provided by Research Resource Network (RRN), Japan. This work was supported by a research grant to J-IS from the High-Tech Research Center Project, the Ministry of Education, Culture, Sports, Science and Technology (MEXT), Japan (S0801043), and from Research on Intractable Diseases, the Ministry of Health, Labour and Welfare of Japan.

References

[1] A. Serretti, P. Olgiati and D. De Ronchi, Genetics of Alzheimer's disease. A rapidly evolving field, *J Alzheimers Dis* **12** (2007), 73–92.

[2] S.F. Kingsmore, I.E. Lindquist, J. Mudge, D.D. Gessler and W.D. Beavis, Genome-wide association studies: progress and potential for drug discovery and development, *Nat Rev Drug Discov* **7** (2008), 221–230.

[3] S.D. Ginsberg, S.E. Hemby, V.M. Lee, J.H. Eberwine and J.Q. Trojanowski, Expression profile of transcripts in Alzheimer's disease tangle-bearing CA1 neurons, *Ann Neurol* **48** (2000), 77–87.

[4] V. Colangelo, J. Schurr, M.J. Ball, R.P. Pelaez, N.G. Bazan and W.J. Lukiw, Gene expression profiling of 12633 genes in Alzheimer hippocampal CA1: transcription and neurotrophic factor down-regulation and up-regulation of apoptotic and pro-inflammatory signaling, *J Neurosci Res* **70** (2002), 462–473.

[5] P. Katsel, C. Li and V. Haroutunian, Gene expression alterations in the sphingolipid metabolism pathways during progression of dementia and Alzheimer's disease: a shift toward ceramide accumulation at the earliest recognizable stages of Alzheimer's disease? *Neurochem Res* **32** (2007), 845–856.

[6] C. Williams, R. Mehrian Shai, Y. Wu, Y.H. Hsu, T. Sitzer, B. Spann, C. McCleary, Y. Mo and C.A. Miller, Transcriptome analysis of synaptoneurosomes identifies neuroplasticity genes overexpressed in incipient Alzheimer's disease, *PLoS ONE* **4** (2009), e4936.

[7] K. Oda, Y. Matsuoka, A. Funahashi and H. Kitano, A comprehensive pathway map of epidermal growth factor receptor signaling, *Mol Syst Biol* **1** (2005), 2005.0010.

[8] F. Noorbakhsh, C.M. Overall and C. Power, Deciphering complex mechanisms in neurodegenerative diseases: the advent of systems biology, *Trends Neurosci* **32** (2009), 88–100.

[9] R. Albert, H. Jeong and A.L. Barabasi, Error and attack tolerance of complex networks, *Nature* **406** (2000), 378–382.

[10] E.M. Blalock, J.W. Geddes, K.C. Chen, N.M. Porter, W.R. Markesbery and P.W. Landfield, Incipient Alzheimer's disease: microarray correlation analyses reveal major transcriptional and tumor suppressor responses, *Proc Natl Acad Sci USA* **101** (2004), 2173–2178.

[11] J.A. Miller, M.C. Oldham and D.H. Geschwind, A systems level analysis of transcriptional changes in Alzheimer's disease and normal aging, *J Neurosci* **28** (2008), 1410–1420.

[12] H. Sato, S. Ishida, K. Toda, R. Matsuda, Y. Hayashi, M. Shigetaka, M. Fukuda, Y. Wakamatsu and A. Itai, New approaches to mechanism analysis for drug discovery using DNA microarray data combined with KeyMolnet, *Curr Drug Discov Technol* **2** (2005) 89–98.

[13] D.W. Huang, B.T. Sherman and R.A. Lempicki, Systematic and integrative analysis of large gene lists using DAVID bioinformatics resources, *Nat Protoc* **4** (2009), 44–57.

[14] E.I. Boyle, S. Weng, J. Gollub, H. Jin, D. Botstein, J.M. Cherry and G. Sherlock, GO: TermFinder – open source software for accessing Gene Ontology information and finding significantly enriched Gene Ontology terms associated with a list of genes, *Bioinformatics* **20** (2004), 3710–3715.

[15] S.S. Mirra, A. Heyman, D. McKeel, S.M. Sumi, B.J. Crain, L.M. Brownlee, F.S. Vogel, J.P. Hughes, G. van Belle and L. Berg, The Consortium to Establish a Registry for Alzheimer's Disease (CERAD). Part II. Standardization of the neuropathologic assessment of Alzheimer's disease, *Neurology* **41** (1991), 479–486.

[16] H. Braak, I. Alafuzoff, T. Arzberger, H. Kretzschmar and K. Del Tredici, Staging of Alzheimer disease-associated neurofibrillary pathology using paraffin sections and immunocytochemistry, *Acta Neuropathol* **112** (2006), 389–404.

[17] T. Misawa, K. Arima, H. Mizusawa and J. Satoh, Close association of water channel AQP1 with amyloid-β deposition in Alzheimer disease brains, *Acta Neuropathol* **116** (2008), 247–260.

[18] B. Mayr and M. Montminy, Transcriptional regulation by the phosphorylation-dependent factor CREB, *Nat Rev Mol Cell Biol* **2** (2001), 599–609.

[19] B.E. Lonze and D.D. Ginty, Function and regulation of CREB family transcription factors in the nervous system, *Neuron* **35** (2002), 605–623.

[20] J. Satoh, Z. Illes, A. Peterfalvi, H. Tabunoki, C. Rozsa and T. Yamamura, Aberrant transcriptional regulatory network in T cells of multiple sclerosis, *Neurosci Lett* **422** (2007), 30–33.

[21] J. Satoh, T. Misawa, H. Tabunoki and T. Yamamura, Molecular network analysis of T-cell transcriptome suggests aberrant regulation of gene expression by NF-κB as a biomarker for relapse of multiple sclerosis, *Dis Markers* **25** (2008), 27–35.

[22] X. Zhang, D.T. Odom, S.H. Koo, M.D. Conkright, G. Canettieri, J. Best, H. Chen, R. Jenner, E. Herbolsheimer, E. Jacobsen, S. Kadam, J.R. Ecker, B. Emerson, J.B. Hogenesch, T. Unterman, R.A. Young and M. Montminy, Genome-wide analysis of cAMP-response element binding protein occupancy, phosphorylation, and target gene activation in human tissues, *Proc Natl Acad Sci USA* **102** (2005), 4459–4464.

[23] H. Viola, M. Furman, L.A. Izquierdo, M. Alonso, D.M. Barros, M.M. de Souza, I. Izquierdo and J.H. Medina, Phosphorylated cAMP response element-binding protein as a molecular marker of memory processing in rat hippocampus: effect of novelty, *J Neurosci* **20** (2000), RC112.

[24] M. Yamamoto-Sasaki, H. Ozawa, T. Saito, M. Rösler and P. Riederer, Impaired phosphorylation of cyclic AMP response element binding protein in the hippocampus of dementia of the Alzheimer type, *Brain Res* **824** (1999), 300–303.

[25] G.S. Griesbach, R.L. Sutton, D.A. Hovda, Z. Ying and F. Gomez-Pinilla, Controlled contusion injury alters molecular systems associated with cognitive performance, *J Neurosci Res* **87** (2009), 795–805.

[26] B. Gong, O.V. Vitolo, F. Trinchese, S. Liu, M. Shelanski and O. Arancio, Persistent improvement in synaptic and cognitive functions in an Alzheimer mouse model after rolipram treatment, *J Clin Invest* **114** (2004), 1624–1634.

[27] Z. Liang, F. Liu, I. Grundke-Iqbal, K. Iqbal and C.X. Gong, Down-regulation of cAMP-dependent protein kinase by over-activated calpain in Alzheimer disease brain, *J Neurochem* **103** (2007), 2462–2470.

[28] D.N. Arvanitis, A. Ducatenzeiler, J.N. Ou, E. Grodstein, S.D. Andrews, S.R. Tendulkar, A. Ribeiro-da-Silva, M. Szyf and A.C. Cuello, High intracellular concentrations of amyloid-β block nuclear translocation of phosphorylated CREB, *J Neurochem* **103** (2007), 216–228.

[29] O.V. Vitolo, A. Sant'Angelo, V. Costanzo, F. Battaglia, O. Arancio and M. Shelanski, Amyloid β-peptide inhibition of the PKA/CREB pathway and long-term potentiation: reversibility by drugs that enhance cAMP signaling, *Proc Natl Acad Sci USA* **99** (2002), 13217–13221.

[30] D. Puzzo, O. Vitolo, F. Trinchese, J.P. Jacob, A. Palmeri and O. Arancio, Amyloid-β peptide inhibits activation of the nitric oxide/cGMP/cAMP-responsive element-binding protein pathway during hippocampal synaptic plasticity, *J Neurosci* **25** (2005), 6887–6897.

[31] Q.L. Ma, M.E. Harris-White, O.J. Ubeda, M. Simmons, W. Beech, G.P. Lim, B. Teter, S.A. Frautschy and G.M. Cole, Evidence of Aβ- and transgene-dependent defects in ERK-CREB signaling in Alzheimer's models, *J Neurochem* **103** (2007), 1594–1607.

[32] Q. Li, H.F. Zhao, Z.F. Zhang, Z.G. Liu, X.R. Pei, J.B. Wang and Y. Li, Long-term green tea catechin administration prevents spatial learning and memory impairment in senescence-accelerated mouse prone-8 mice by decreasing $A\beta_{1-42}$ oligomers and upregulating synaptic plasticity-related proteins in the hippocampus, *Neuroscience* (2009), in press, doi:10.1016/j.neuroscience.2009.07.014.

[33] F.G. De Felice, A.P. Wasilewska-Sampaio, A.C. Barbosa, F.C. Gomes, W.L. Klein and S.T. Ferreira, Cyclic AMP enhancers and Aβ oligomerization blockers as potential therapeutic agents in Alzheimer's disease, *Curr Alzheimer Res* **4** (2007), 263–271.

[34] R.A. Nixon, Autophagy, amyloidogenesis and Alzheimer disease, *J Cell Sci* **120** (2007), 4081–4091.

[35] C.V. Garat, D. Fankell, P.F. Erickson, J.E. Reusch, N.N. Bauer, I.F. McMurtry and D.J. Klemm, Platelet-derived growth factor BB induces nuclear export and proteasomal degradation of CREB via phosphatidylinositol 3-kinase/Akt signaling in pulmonary artery smooth muscle cells, *Mol Cell Biol* **26** (2006), 4934–4948.

[36] S. Costes, B. Vandewalle, C. Tourrel-Cuzin, C. Broca, N. Linck, G. Bertrand, J. Kerr-Conte, B. Portha, F. Pattou, J. Bockaert and S. Dalle, Degradation of cAMP-responsive element-binding protein by the ubiquitin-proteasome pathway contributes to glucotoxicity in beta-cells and human pancreatic islets, *Diabetes* **58** (2009) 1105–1115.

[37] K. Okamoto, S. Hirai, T. Iizuka, T. Yanagisawa and M. Watanabe, Reexamination of granulovacuolar degeneration, *Acta Neuropathol* **82** (1991), 340–345.

[38] C. Stadelmann, T.L. Deckwerth, A. Srinivasan, C. Bancher, W. Brück, K. Jellinger and H. Lassmann, Activation of caspase-3 in single neurons and autophagic granules of granulovacuolar degeneration in Alzheimer's disease. Evidence for apoptotic cell death, *Am J Pathol* **155** (1999), 1459–1466.

[39] K. Leroy, A. Boutajangout, M. Authelet, J.R. Woodgett, B.H. Anderton and J.P. Brion, The active form of glycogen synthase kinase-3β is associated with granulovacuolar degeneration in neurons in Alzheimer's disease, *Acta Neuropathol* **103** (2002), 91–99.

[40] S. Lagalwar, R.W. Berry and L.I. Binder, Relation of hippocampal phospho-SAPK/JNK granules in Alzheimer's disease and tauopathies to granulovacuolar degeneration bodies, *Acta Neuropathol* **113** (2007), 63–73.

[41] A. Thakur, X. Wang, S.L. Siedlak, G. Perry, M.A. Smith and X. Zhu, c-Jun phosphorylation in Alzheimer disease, *J Neurosci Res* **85** (2007), 1668–1673.

[42] J.J. Hoozemans, E.S. van Haastert, D.A. Nijholt, A.J. Rozemuller, P. Eikelenboom and W. Scheper, The unfolded protein response is activated in pretangle neurons in Alzheimer's disease hippocampus, *Am J Pathol* **174** (2009), 1241–1251.

[43] A. Kadokura, T. Yamazaki, S. Kakuda, K. Makioka, C.A. Lemere, Y. Fujita, M. Takatama and K. Okamoto, Phosphorylation-dependent TDP-43 antibody detects intraneuronal dot-like structures showing morphological characters of granulovacuolar degeneration, *Neurosci Lett* (2009), in press, doi:10.1016/j.neulet.2009.06.024.

[44] D.W. Dickson, H. Ksiezak-Reding, P. Davies and S.H. Yen, A monoclonal antibody that recognizes a phosphorylated epitope in Alzheimer neurofibrillary tangles, neurofilaments and tau proteins immunostains granulovacuolar degeneration, *Acta Neuropathol* **73** (1987), 254–258.

[45] W. Bondareff, C.M. Wischik, M. Novak and M. Roth, Sequestration of tau by granulovacuolar degeneration in Alzheimer's disease, *Am J Pathol* **139** (1991), 641–647.

[46] B. Boland, A. Kumar, S. Lee, F.M. Platt, J. Wegiel, W.H. Yu and R.A. Nixon, Autophagy induction and autophagosome clearance in neurons: relationship to autophagic pathology in Alzheimer's disease, *J Neurosci* **28** (2008) 6926–6937.

[47] W.Y. Ong, H.M. Lim, T.M. Lim and B. Lutz, Kainate-induced neuronal injury leads to persistent phosphorylation of cAMP response element-binding protein in glial and endothelial cells in the hippocampus, *Exp Brain Res* **131** (2000), 178–186.

[48] L.J. Cox, U. Hengst, N.G. Gurskaya, K.A. Lukyanov and S.R. Jaffrey, Intra-axonal translation and retrograde trafficking of CREB promotes neuronal survival, *Nat Cell Biol* **10** (2008) 149–159.

[49] I Granic, A.M. Dolga, I.M. Nijholt, G. van Dijk and U.L. Eisel, Inflammation and NF-κB in Alzheimer's disease and diabetes, *J Alzheimers Dis* **16** (2009), 809–821.

[50] K. Terai, A. Matsuo and P.L. McGeer, Enhancement of immunoreactivity for NF-κB in the hippocampal formation and cerebral cortex of Alzheimer's disease, *Brain Res* **735** (1996), 159–168.

[51] W.J. Lukiw, Y. Zhao and J.G. Cui, An NF-κB-sensitive micro RNA-146a-mediated inflammatory circuit in Alzheimer

disease and in stressed human brain cells, *J Biol Chem* **283** (2008), 31315–31322.

[52] D. Gezen-Ak, E. Dursun, T. Ertan, H. Hanağasi, H. Gürvit, M. Emre, E. Eker, M. Oztürk, F. Engin and S. Yilmazer, Association between vitamin D receptor gene polymorphism and Alzheimer's disease, *Tohoku J Exp Med* **212** (2007), 275–282.

[53] M.K. Sutherland, M.J. Somerville, L.K. Yoong, C. Bergeron, M.R. Haussler and D.R. McLachlan, Reduction of vitamin D hormone receptor mRNA levels in Alzheimer as compared to Huntington hippocampus: correlation with calbindin-28k mRNA levels, *Brain Res Mol Brain Res* **13** (1992), 239–250.

NEUROPATHOLOGY

Neuropathology 2010; **30**, 7–14 doi:10.1111/j.1440-1789.2009.01035.x

Original Article

Protein microarray analysis identifies cyclic nucleotide phosphodiesterase as an interactor of Nogo-A

Kenta Sumiyoshi,[1] Shinya Obayashi,[1] Hiroko Tabunoki,[1] Kunimasa Arima[2] and Jun-ichi Satoh[1]

[1]Department of Bioinformatics and Molecular Neuropathology, Meiji Pharmaceutical University, and [2]Department of Psychiatry, National Center Hospital, NCNP, Tokyo, Japan

Nogo-A, a neurite outgrowth inhibitor, is expressed exclusively on oligodendrocytes and neurons in the CNS. The central domain of Amino-Nogo spanning amino acids 567–748 in the human Nogo-A designated NIG, mediates persistent inhibition of axonal outgrowth and induces growth cone collapse by signaling through an as yet unidentified NIG receptor. We identified 82 NIG-interacting proteins by screening a high-density human protein microarray composed of 5000 proteins with a recombinant NIG protein as a probe. Following an intensive database search, we selected 12 neuron/oligodendrocyte-associated NIG interactors. Among them, we verified the molecular interaction of NIG with 2′, 3′-cyclic nucleotide 3′-phosphodiesterase (CNP), a cell type-specific marker of oligodendrocytes, by immunoprecipitation and cell imaging analysis. Although CNP located chiefly in the cytoplasm of oligodendrocytes might not serve as a cell-surface NIG receptor, it could act as a conformational stabilizer for the intrinsically unstructured large segment of Amino-Nogo.

Key words: CNP, NIG, Nogo-A, protein microarray, protein-protein interaction.

INTRODUCTION

Nogo is a family of myelin-associated inhibitors for axonal regeneration in the CNS.[1] It consists of three isoforms named A, B and C, all of which share a C-terminal 66 amino acid segment named Nogo-66. Nogo-A, the longest isoform with the strongest activity of neurite outgrowth inhibition, is expressed exclusively in myelin sheaths and oligodendrocytes on the cell surface and in the endoplasmic reticulum (ER), in addition to a subpopulation of neurons in the adult CNS. Nogo-A also plays a key role in maturation of oligodendrocytes *in vivo*.[2] Nogo-B is ubiquitously distributed both inside and outside the CNS, while Nogo-C, the shortest isoform, is enriched in skeletal muscle. Nogo-A has at least two discrete domains that exhibit neuronal growth-inhibitory activities.[3] One is located in the Nogo-A-specific C-terminal segment of Amino-Nogo, and the other is Nogo-66. The N-terminal segment of Amino-Nogo, shared between Nogo-A and Nogo-B, plays a role in vascular remodeling. Nogo-66, along with oligodendrocyte-myelin glycoprotein (OMgp) and myelin-associated glycoprotein (MAG), transduces inhibitory signals via a molecular complex composed of the Nogo receptor (NgR), Lingo-1, and $p75^{NTR}$ or Troy by activating RhoA that mediates actin depolymerization responsible for the collapse of growth cones on regenerating axons.[1]

The Nogo-A-specific C-terminal segment of Amino-Nogo, being conformationally unfolded,[4,5] mediates persistent inhibition of axonal outgrowth and induces growth cone collapse via the NgR-independent mechanism.[6] The central region of this segment spanning amino acids 567–748 in the human Nogo-A designated NIG, is pivotal for this activity.[3] Because the NIG domain exists only in Nogo-A, it provides an explanation for Nogo-A acting as the most potent inhibitor of axonal growth among three Nogo isoforms. Importantly, treatment with the antibody raised against the Nogo-A-specific domain enhances sprouting of corticospinal axons and promotes functional recovery following spinal cord injury in adult primates.[7] A previous study showed that the predominant proteins that

Correspondence: Jun-ichi Satoh, MD, Department of Bioinformatics and Molecular Neuropathology, Meiji Pharmaceutical University, 2-522-1 Noshio, Kiyose, Tokyo 204-8588, Japan. Email: satoj@my-pharm.ac.jp

Received 18 March 2009; Revised 13 April 2009; Accepted 14 April 2009; published online 7 June 2009.

interact with Nogo-A are Nogo-B and Nogo-C.[8] Although Amino-Nogo interacts with α5 and αv integrins,[9] the NIG-specific receptor remains to be characterized.

Recently, protein microarray technology has been established for rapid and systematic screening of protein-protein interactions in a high-throughput fashion.[10] The protein microarray is a chip on which thousands of functional proteins are immobilized. By reacting the array with the specific protein as a probe, it enables us to efficiently identify the target protein on chip as a binding partner. Protein microarray has a wide range of applications, including characterization of antibody specificity and autoantibody repertoire, and identification of novel biomarkers and molecular targets associated with disease type, stage and progression.[10] In the present study, we attempted to characterize a comprehensive profile of NIG-interacting proteins, which might include a candidate for NIG receptors, by using the high-density human protein microarray.

MATERIALS AND METHODS

Protein microarray analysis

We utilized ProtoArray v3.0 (Invitrogen, Carlsbad, CA, USA) that contains 5000 recombinant glutathione S-transferase (GST)-tagged human proteins expressed by the baculovirus expression system. They are purified to ensure the preservation of native structure, post-translational modifications, and proper functionality, as described previously.[11,12] The target proteins cover a wide range of biologically important proteins, and the complete list is shown in Table S1 online. The proteins are spotted on the glass slide in an arrangement of 4 × 12 subarrays equally spaced in vertical and horizontal directions. Because target proteins on the array protrude from the surface via N-terminal GST serving as a spacer, the probe is spatially accessible to all parts of them. Each subarray includes 20 × 20 spots, composed of 76 positive and negative control spots, 222 human target proteins, and 102 blanks and empty spots.

To prepare the probe for microarray analysis, the gene encoding the human NIG domain (NM_020532) was amplified by PCR with the primer set of 5′actggtacaaagat tgcttatgaa3′ and 5′aaataagtcaactggttcagaatc3′. It is worthy to note that the amino acid sequence of human NIG shows 82% and 80% identity to the rat or mouse ortholog, respectively. The PCR product was first cloned into the vector pSecTag/FRT/V5-His-TOPO (Invitrogen). Then, the gene segment coding for V5-tagged NIG was transferred into the vector pTrcHis-TOPO (Invitrogen). The V5-tagged NIG protein was expressed in *E. coli* and purified from the lysate by passing through the histidine-tagged proteins (HIS)-select spin column (Sigma, St. Louis, MO, USA), as described previously.[11,12] The purity and specificity of the probe were verified by silver stain and Western blot with mouse monoclonal anti-V5 antibody (Invitrogen) and sheep polyclonal anti-human NIG antibody (AF3515; R&D Systems, Minneapolis, MN, USA).

To block non-specific binding, the array was incubated at 4°C for 1 h with the phosphate-buffered saline supplemented with Tween 20 (PBST) blocking buffer, composed of 1% bovine serum albumin (BSA) and 0.1% Tween 20 in phosphate-buffered saline (PBS). Then, the array was incubated at 4°C for 90 min with the probe described above at a concentration of 100 μg/mL in the probing buffer, according to the methods described previously.[11,12] The array was then incubated at 4°C for 30 min with Alexa Fluor 647-conjugated mouse monoclonal anti-V5 antibody (Invitrogen). After washing, it was scanned by the GenePix 4200A scanner (Axon Instruments, Union City, CA, USA) at a wavelength of 635 nm. The data were analyzed by using the ProtoArray Prospector software v4.0 (Invitrogen), following acquisition of the microarray lot-specific information that compensates inter-lot variations among arrays in protein concentrations identified by the post-printing quality control. The spots showing the background-subtracted signal intensity value greater than the median plus three standard deviations of all the fluorescence intensities were considered as having significant interactions. The Z-score was calculated as the background-subtracted signal intensity value of the target protein minus the average of the background-subtracted signal intensity value from the negative control distribution, divided by the standard deviation of the negative control distribution. The cut-off value of Z-score was set as 3, as described previously.[11,12]

Immunoprecipitation and Western blot analysis

The coimmunoprecipitation analysis was performed according to the methods described previously.[11,12] In brief, the protein extract was prepared from the cells and tissues solubilized in mammalian protein extraction reagent (M-PER) protein extraction buffer (Pierce, Rockford, IL, USA). After preclearance, it was processed for immunoprecipitation with rabbit polyclonal anti-Nogo-A antibody (H-300; Santa Cruz Biotechnology, Santa Cruz, CA, USA) or rabbit polyclonal anti-2′, 3′-cyclic nucleotide 3′-phosphodiesterase (CNP) antibody (M-300; Santa Cruz Biotechnology). The precipitates were then processed for Western blot with anti-NIG antibody (AF3515) or mouse monoclonal anti-CNP antibody (11-5B; Sigma). The negative control included normal rabbit IgG instead of specific antibodies during the immunoprecipitation process. The specific reaction was visualized by using a chemiluminescence substrate (Pierce).

To specify the CNP-interacting domain of Nogo-A, the protein extract of HEK293 cells, in which the transgenes encoding NIG and CNP were coexpressed, was processed for coimmunoprecipition analysis. To achieve this, the NIG gene or the full-length CNP gene was amplified by PCR, and cloned into the expression vector p3XFLAG-CMV7.1 (Sigma) or pCMV-Myc (Clontech, Mountain View, CA, USA) to express a fusion protein with an N-terminal Flag or Myc tag, respectively. After cotransfection of the vectors in HEK293 cells, the protein extract was processed for immunoprecipitation with mouse monoclonal anti-Flag M2 affinity gel (Sigma) or rabbit polyclonal anti-Myc-conjugated agarose (Sigma). This was followed by Western blot with rabbit polyclonal anti-Myc antibody (Sigma) and mouse monoclonal anti-FLAG M2 antibody (Sigma).

Cell imaging, immunocytochemistry and immunohistochemistry

To determine coexpression of NIG and CNP in neural cell cultures, the NIG gene or the full-length CNP was cloned into the expression vector pDsRed-Express-C1 (Clontech) or pFN2A CMV Flexi (Promega, Madison, WI, USA) to express a fusion protein with an N-terminal DsRed or Halo tag, respectively. They were cotransfected in SK-N-SH neuroblastoma cells. At 24–48 h after transfection, the cells were exposed to Oregon Green (Promega), a fluorochrome specifically bound to the Halo tag protein. In some experiments, primary cultures established from the brain of newborn Institute of Cancer Research (ICR) mice were processed for double-immunolabeling with anti-NIG antibody (AF3515) and anti-CNP antibody (11-5B), followed by labeling with Alexa Fluor 568-conjugated anti-sheep IgG (Invitrogen) and Alexa Fluor 488-conjugated anti-mouse IgG (Invitrogen). Subsequently, the cells were fixed briefly in 4% paraformaldehyde, exposed to 4′, 6′-diamidino-2-phenylindole (DAPI; Invitrogen), mounted on slides with glycerol-polyvinyl alcohol, and examined on the Olympus BX51 universal microscope.

For double-labeling immunohistochemistry, deparaffinated tissue sections were heated in 10 mmol/L citrate sodium buffer, pH 6.0 by autoclave for 30 s at 125°C in a temperature-controlled pressure chamber (Dako, Tokyo, Japan). They were incubated with PBS containing 10% normal goat serum for 15 min at room temperature (RT) to block non-specific staining. Then, tissue sections were stained at RT overnight with anti-CNP antibody (11-5B), followed by incubation with alkaline phosphatase (AP)-conjugated anti-mouse IgG (Nichirei, Tokyo, Japan), and colorized with New Fuchsin substrate. After inactivation of the antibody by autoclaving the sections at 125°C for 30 s in 10 mM citrate sodium buffer, pH 6.0, the tissue sections were treated for 15 min with 3% hydrogen peroxide-containing distilled water to block the endogenous peroxidase activity. Then, they were relabeled with anti-Nogo-A antibody (H-300) or anti-NIG antibody (AF-3515), followed by incubation with horseradish peroxidase (HRP)-conjugated secondary antibodies, and colorized with DAB substrate and a counterstain with hematoxylin. For negative controls, the step of incubation with primary antibodies was omitted.

RESULTS

Protein microarray-identified 82 NIG interactors

For protein microarray analysis, we prepared a highly purified V5-tagged NIG probe showing a single 45-kDa band in a 12% SDS-PAGE gel (Fig. 1a, lanes 1–3). By screening the protein microarray with this probe, we identified 82 proteins as those showing significant interaction with NIG among 5000 proteins on the array. They are listed in Table S2 online. Because Nogo-A is located not only on the plasma membrane of oligodendrocytes, but also in the ER where the NIG domain is exposed to the cytosol,[13] it is not surprising that many extramembrane proteins are listed in NIG-interacting partners.

Selection of CNP as the most probable NIG interactor candidate

First, for 82 NIG interactors, we investigated the EST profile on UniGene (http://www.ncbi.nlm.nih.gov/UniGene), the protein expression profile on Human Protein Reference Database (HPRD; http://www.hprd.org), and the mRNA expression profile of mouse orthologs in the brain on the Allen Brain Atlas (ABA) database (http://www.brain-map.org), a high-throughput *in situ* hybridization atlas of gene expression pattern in the adult mouse brain.[14] The database search suggested that the great majority of 82 NIG interactors represent non-neural proteins, suggesting the promiscuous binding of most NIG interactors in a non-physiological setting on the array. Therefore, we focused exclusively on the proteins whose expression in the CNS is supported by the expression profiling on UniGene, HRPD and ABA databases. Subsequently, we identified the proteins highly relevant to the biological function of Nogo-A by searching on PubMed by importing brain, neuron, neurite, axon, myelin, or oligodendrocyte as search terms. Following intensive search, we retrieved 12 neuron/oligodendrocyte-associated NIG interactors that were hit by any of these key words (Table 1). Among them, we finally found that only CNP (the spots in Fig. 1b), a cell type-specific marker for oligodendrocytes, has a physiological relevance to axon, myelin and oligodendrocytes (see the details in the Discussion section).

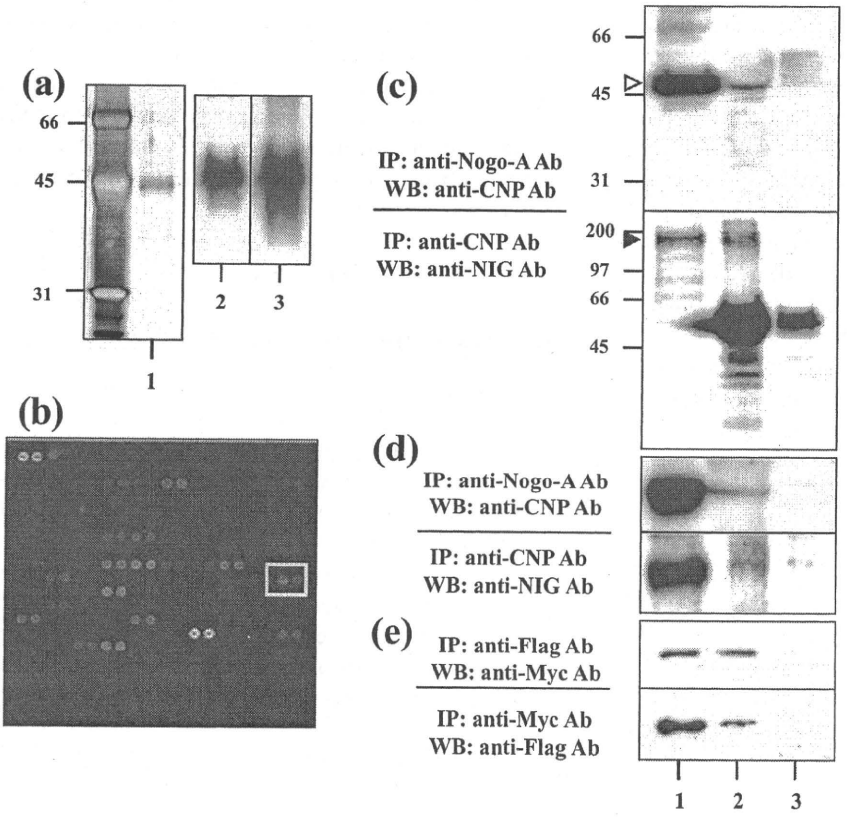

Fig. 1 Protein microarray and immunoprecipitation analysis. (a) The V5-tagged NIG-specific probe utilized for microarray analysis. The probe (0.3 μg each lane) was separated by a 12% SDS-PAGE gel. The silver stain of the gel with the position of molecular weight markers (lane 1). The blot was labeled with anti-V5 antibody (lane 2) and anti-human NIG antibody (lane 3). (b) Anti-2′, 3′-cyclic nucleotide 3′-phosphodiesterase (CNP) identified as a NIG interactor on the array. The protein microarray containing duplicate spots of 5000 proteins is composed of 4 × 12 subarrays. Each subarray includes 20 × 20 spots, composed of 76 control spots, including 14 positive and 62 negative control spots, 222 human target proteins, and 102 blanks and empty spots. The subarray No. 20 is shown. The spots positioned at row 10, columns 19, 20 indicated by an enclosed yellow line represent CNP. (c–e) Immunoprecipitation (IP) and Western blot (WB). Anti-Nogo-A antibody pulled down the endogenous CNP (open arrow, 47-kDa), while anti-CNP antibody precipitated the endogenous full-length Nogo-A (filled arrow, 190-kDa) from (c) the human brain homogenate, and from (d) the rat C6 glioma cell lysate. (e) The NIG gene and the CNP gene were cloned into the expression vectors to express a fusion protein with a Flag or Myc tag, respectively. They were cotransfected in HEK293 cells, and the lysate was processed for immunoprecipitation analysis with anti-Flag antibody and anti-Myc antibody. The lanes (1–3) of (c–e) represent (1) input control, (2) IP with the target-specific antibody, and (c) IP with normal mouse or rabbit IgG.

Validation of the interaction between NIG and CNP

Next, we verified the molecular interaction between Nogo-A and CNP by coimmunoprecipitation analysis. Anti-Nogo-A antibody (H-300) pulled down the endogenous CNP (47-kDa) labeled with anti-CNP antibody, while anti-CNP antibody (M-300) precipitated the full-length Nogo-A (190-kDa) labeled with anti-NIG antibody from both the human brain homogenate and the lysate of rat C6 glioma cells (Fig. 1c,d, upper and lower panels, lane 2). In contrast, the inclusion of normal IgG instead of H-300 or M-300 antibody recovered neither CNP nor Nogo-A (Fig. 1c,d, upper and lower panels, lane 3), supporting the specificity of the interaction. These results indicate that the endogenous Nogo-A interacts with the endogenous CNP *in vitro* and *in vivo*.

To specify the CNP-interacting domain of Nogo-A, the NIG gene or the CNP gene was cloned into the two different expression vectors to express a fusion protein with an N-terminal Flag or Myc tag. After cotransfection of the vectors in HEK293 cells, the protein extract was processed for immunoprecipitation with mouse monoclonal anti-Flag M2 affinity gel, rabbit polyclonal anti-Myc-conjugated agarose, or the same amount of normal mouse or rabbit IgG-conjugated agarose, followed by Western blot with rabbit polyclonal anti-Myc antibody and mouse monoclonal anti-FLAG M2 antibody. The reciprocal coimmunoprecipitation analysis verified the interaction of the NIG domain of Nogo-A and CNP (Fig. 1e, upper and lower panels, lane 2). These results indicate that the NIG domain of Nogo-A on its own interacts with CNP, but do not exclude the possibility that the domain located outside NIG is also bound to CNP.

To determine subcellular colocation of NIG and CNP, the NIG gene or the CNP gene was cloned into the two different expression vectors to express a fusion protein with an N-terminal DsRed or Halo tag. When cotransfected in SK-N-SH neuroblastoma cells, NIG was expressed not only on the plasma membrane but also in the cytoplasm, and at low amounts in the nucleus. DsRed-tagged NIG and Oregon Green-labeled CNP were coexpressed chiefly in the cytoplasm (Fig. 2, panels a–c). Furthermore, coexpression of NIG and CNP was identified

Table 1 Twelve neuron/oligodendrocyte-associated NIG interactors

No.	Gene symbol	Gene name	Z-score	Putative function
1	RPL31	Ribosomal protein L31	7.22386	A ribosomal protein that constitutes a component of the 60S subunit
2	CIRBP	Cold inducible RNA binding protein	6.76639	A cold-shock protein that plays a role in cold-induced suppression of cell proliferation
3	PLK3	Polo-like kinase 3 (Drosophila)	6.51572	A serine/threonine kinase that plays a role in regulation of cell cycle progression
4	MARK4	MAP/microtubule affinity-regulating kinase 4	5.45038	A serine/threonine kinase involved in microtubule organization in neuronal cells
5	RPL30	Ribosomal protein L30	4.82371	A ribosomal protein that constitutes a component of the 60S subunit
6	CNP	2′,3′-cyclic nucleotide 3′ phosphodiesterase	4.71717	A membrane-bound enzyme located in the CNS myelin
7	FGF13	Fibroblast growth factor 13	4.35684	A member of the fibroblast growth factor family
8	ZNF192	Zinc finger protein 192	4.09363	A transcription factor of unknown function
9	NHP2	Nucleolar protein family A, member 2 (H/ACA small nucleolar RNPs)	4.04663	A member of the H/ACA snoRNPs gene family
10	ATP5O	ATP synthase, H+ transporting, mitochondrial F1 complex, O subunit (oligomycin sensitivity conferring protein)	3.25389	A component of the F-type ATPase located in the mitochondrial matrix
11	ODC1	Ornithine decarboxylase 1	3.06902	The rate-limiting enzyme of the polyamine biosynthesis pathway that catalyzes ornithine to putrescine
12	EIF2C1	Eukaryotic translation initiation factor 2C, 1	3.00322	A member of the Argonaute family that plays a role in RNA interference

Among 82 NIG interactor candidates (Table S2), 12 were categorized as neuron/oligodendrocyte-associated NIG interactors by database search on UniGene, HPRD, and Allen Brain Atlas, and by the PubMed search with brain, neuron, neurite, axon, myelin, or oligodendrocyte as search terms. Among them, we found that only CNP (No. 6) has a physiological relevance to axon, myelin and oligodendrocytes.

both in the cytoplasm and on the cell surface of highly-branched differentiated oligodendrocytes consisting of a small population of newborn mouse brain cell cultures (Fig. 2, panels d–f).

Finally, we studied coexpression of Nogo-A and CNP *in vivo* in the human brain by immunohistochemistry. A substantial overlap was found in the expression pattern of Nogo-A, NIG and CNP in oligodendrocytes and myelin sheaths of the cerebral white matter (Fig. 2, panels g and h), supporting the possibility that Nogo-A *in vivo* interacts with CNP, probably by binding via the NIG domain.

DISCUSSION

Protein microarray serves as a powerful tool for the rapid and systematic identification of protein-protein and other biomolecule interactions.[10] Protein microarray has a wide range of applications, including characterization of antibody specificity and autoantibody repertoire, and identification of novel biomarkers and molecular targets associated with disease type, stage and progression, leading to establishment of personalized medicine.[10] When a specific probe is available, the whole experimental procedure of protein microarray analysis requires the exact time shorter than 5 h to obtain the complete list of interacting proteins on the array.[11,12]

However, protein microarray technology is still under development in methodological aspects.[10–12] In general, protein microarray has its own limitations associated with the expression and purification of a wide variety of target proteins. In the microarray we utilized, the target proteins were expressed in a baculovirus expression system, purified under native conditions, and spotted on the slides to ensure the preservation of native structure, post-translational modifications such as glycosylation and phophorylation, and proper functionality. In contrast, bacterially expressed proteins lack glycosylation and phosphorylation moieties, and are often misfolded during purification. Since target proteins contain a GST fusion tag, the arrays are always processed for the post-spotting quality control by using an anti-GST antibody with a concentration gradient of GST spots as a standard. This procedure makes it possible to quantify the exact amount of proteins deposited in each spot, and thereby minimizes the inter-lot variability of the results. Furthermore, each subarray contains a series of built-in control spots.

Protein microarray also has another technical limitation attributable to the avidity of protein-protein interaction.[10–12] The probing and rigorous washing procedure detects mostly the direct protein-protein interaction supported by the stable binding ability. It could not efficiently detect much weak and transient protein-protein interactions, or indirect interactions that require accessory molecules or intervening cofactors. In addition,

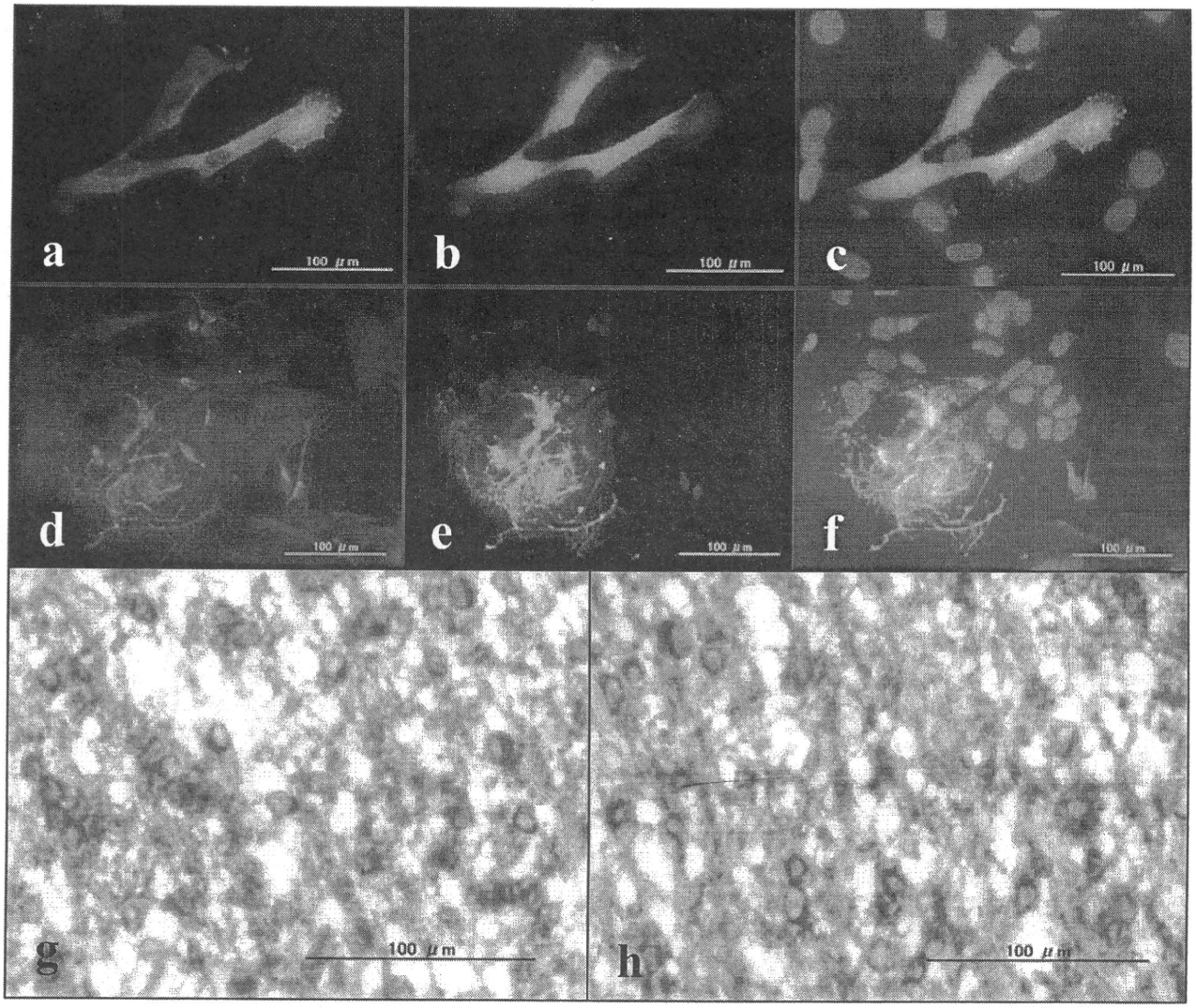

Fig. 2 Coexpression of NIG and anti-2′, 3′-cyclic nucleotide 3′-phosphodiesterase (CNP). (a–c) SK-N-SH neuroblastoma cells. The NIG gene and the CNP gene were cloned into the expression vectors to express a fusion protein with a DsRed or Halo tag, and they were cotransfected in SK-N-SH cells. (a) DsRed-labeled NIG, (b) Oregon Green-labeled CNP, and (c) merge (a) and (b) with 4′, 6′-diamidino-2-phenylindole (DAPI). (d–f) Newborn mouse brain cell cultures. Primary cultures established from newborn ICR mice double immunolabeled with anti-NIG antibody (AF3515) and anti-CNP antibody (11-5B), followed by labeling with Alexa Fluor 568-conjugated anti-sheep IgG and Alexa Fluor 488-conjugated anti-mouse IgG. (d) NIG, (e) CNP, and (f) merge (d) and (e) with DAPI. (g,h) Human brain tissues. The human brain tissue section derived from the peri-infarct white matter of the frontal cortex of a 62-year-old male with middle cerebral artery occlusion was double immunolabeled with (g) anti-Nogo-A antibody (H-300; brown) and anti-CNP antibody (11-5B; red) and (h) anti-NIG antibody (AF3515; brown) and anti-CNP antibody (11-5B; red).

protein microarray screening does not consider the specific subcellular location where the protein-protein interaction actually takes place. Thus, it is possible that some promiscuous partners are detected, whereas some biologically important interactors *in vivo* are left beyond identification. Therefore, protein microarray data always require the validation by other independent methods such as coimmunoprecipitation, Western blotting, the yeast two-hybrid (Y2H) screening, and so on. Post-translational modifications play a pivotal role in a range of protein-protein interactions. Immunolabeling of the array we utilized with anti-phosphotyrosine antibody showed that approximately 10–20% of the proteins on the array are phosphorylated (unpublished data of Invitrogen). When the array was applied for kinase substrate identification, most known kinases immobilized on the array are enzymatically active with the capacity of autophosphorylation, suggesting that they are functionally

active with preservation of proper conformation (unpublished data of Invitrogen).

Previous studies indicate that the central domain of Amino-Nogo spanning amino acids 567–748 in the human Nogo-A designated NIG mediates persistent inhibition of axonal outgrowth and induces growth cone collapse by signaling through an as yet unidentified NIG receptor.[3] To characterize NIG-interacting proteins that might include an NIG receptor, we screened the high-density human protein microarray composed of 5000 proteins with a recombinant NIG protein as a probe. However, most of the 82 NIG interactors identified by protein microarray analysis are non-neural proteins, suggesting promiscuous binding in a non-physiological setting on the array. Therefore, we focused exclusively on the proteins whose expression in the CNS is supported by the expression profiling on UniGene, HRPD and ABA databases. Subsequently, we searched them on PubMed and retrieved 12 neuron/oligodendrocyte-associated NIG interactors (Table 1). Among them, we finally identified CNP as the most probable candidate in view of a physiological relevance to axon, myelin and oligodendrocytes. CNP is a valid cell type-specific marker for oligodendrocytes, essential for axonal support but not for myelin assembly.[15] CNP acts as a membrane anchor for tubulin required for process outgrowth of oligodendrocytes,[16,17] and ubiquitinated CNP is concentrated within lipid rafts,[18] suggesting that CNP expressed intracellularly in the cytoplasm is located in close proximity to the cell membrane where Nogo-A is accumulated. Therefore, we considered CNP as the most feasible NIG interactor candidate *in vivo*. The interaction of NIG with CNP and their coexpression in both oligodendrocytes and myelin were validated by immunoprecipitation, cell imaging, and immunolabeling.

Previously, we and others showed that Nogo-A expression is greatly enhanced in surviving oligodendrocytes and CNP is expressed in damaged but still remaining myelin sheaths, while NgR is upregulated in reactive astrocytes and macrophages/microglia at the edge of chronic active demyelinating lesions of multiple sclerosis (MS),[19,20] suggesting a pathological role of Nogo-A/NgR interaction in persistent demyelination and loss of axonal regeneration in MS lesions. Interestingly, a certain population of MS patients shows enhanced T-cell and B-cell responses against CNP and Nogo-A, suggesting that both CNP and Nogo-A serve as autoantigens.[21,22] Nogo-A takes at least two different membrane topologies in oligodendrocytes,[3,8] where it is possible that the N-terminal region of Nogo-A is exposed to the extracellular space or is located in the cytoplasm. Because CNP is expressed primarily in the cytoplasm of oligodendrocytes, it might not serve as a cell-surface NIG receptor possibly expressed on axons and

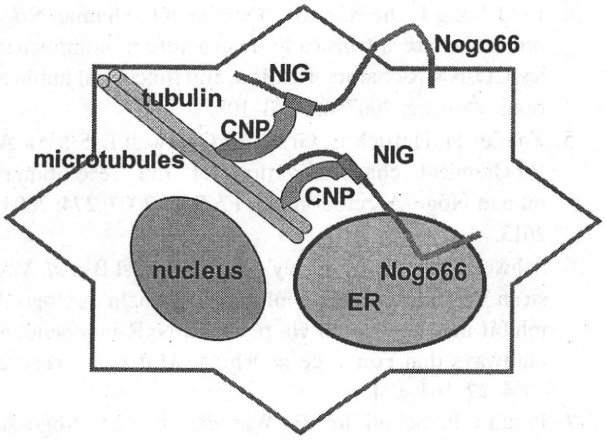

Fig. 3 A hypothetical model of NIG and anti-2′, 3′-cyclic nucleotide 3′-phosphodiesterase (CNP) interaction in oligodendrocytes. CNP (the orange piece) acts as a membrane anchor for tubulin essential for process outgrowth of oligodendrocytes, located in close proximity to the plasma membrane and possibly to the ER membrane where Nogo-A is accumulated. By interacting with NIG (the grey box), CNP serves as an intracellular conformational stabilizer for the intrinsically unstructured large segment of Amino-Nogo.

neurons that transduces the signals for inhibition of axonal outgrowth and induction of growth cone collapse. However, the possibility exists that CNP could act as an intracellular conformational stabilizer for the intrinsically-unstructured unstable Amino-Nogo segment in oligodendrocytes (Fig. 3).

ACKNOWLEDGMENTS

All autopsied brain samples obtained under written informed consent were provided by Research Resource Network (RRN), Japan. This work was supported by a research grant to J-IS from the High-Tech Research Center Project, the Ministry of Education, Culture, Sports, Science and Technology (MEXT), Japan (S0801043).

REFERENCES

1. Walmsley AR, Mir AK. Targeting the Nogo-a signalling pathway to promote recovery following acute CNS injury. *Curr Pharm Des* 2007; **13**: 2470–2484.
2. Pernet V, Joly S, Christ F, Dimou L, Schwab ME. Nogo-A and myelin-associated glycoprotein differently regulate oligodendrocyte maturation and myelin formation. *J Neurosci* 2008; **28**: 7435–7444.
3. Oertle T, van der Haar ME, Bandtlow CE *et al.* Nogo-A inhibits neurite outgrowth and cell spreading with three discrete regions. *J Neurosci* 2003; **23**: 5393–5406.

4. Li M, Song J. The N- and C-termini of the human Nogo molecules are intrinsically unstructured: bioinformatics, CD, NMR characterization, and functional implications. *Proteins* 2007; **68**: 100–108.
5. Zander H, Hettich E, Greiff K, Chatwell L, Skerra A. Biochemical characterization of the recombinant human Nogo-A ectodomain. *FEBS J* 2007; **274**: 2603–2613.
6. Schweigreiter R, Walmsley AR, Niederöst B *et al.* Versican V2 and the central inhibitory domain of Nogo-A inhibit neurite growth via p75NTR/NgR-independent pathways that converge at RhoA. *Mol Cell Neurosci* 2004; **27**: 163–174.
7. Freund P, Schmidlin E, Wannier T *et al.* Nogo-A-specific antibody treatment enhances sprouting and functional recovery after cervical lesion in adult primates. *Nat Med* 2006; **12**: 790–792.
8. Dodd DA, Niederoest B, Bloechlinger S, Dupuis L, Loeffler JP, Schwab ME. Nogo-A, -B, and -C are found on the cell surface and interact together in many different cell types. *J Biol Chem* 2005; **280**: 12494–12502.
9. Hu F, Strittmatter SM. The N-terminal domain of Nogo-A inhibits cell adhesion and axonal outgrowth by an integrin-specific mechanism. *J Neurosci* 2008; **28**: 1262–1269.
10. Schweitzer B, Predki P, Snyder M. Microarrays to characterize protein interactions on a whole-proteome scale. *Proteomics* 2003; **3**: 2190–2199.
11. Satoh J, Nanri Y, Yamamura T. Rapid identification of 14-3-3-binding proteins by protein microarray analysis. *J Neurosci Methods* 2006; **152**: 278–288.
12. Satoh J, Obayashi S, Misawa T, Sumiyoshi K, Oosumi K, Tabunoki H. Protein microarray analysis identifies human cellular prion protein interactors. *Neuropathol Appl Neurobiol* 2009; **35**: 16–35.
13. Voeltz GK, Prinz WA, Shibata Y, Rist JM, Rapoport TA. A class of membrane proteins shaping the tubular endoplasmic reticulum. *Cell* 2006; **124**: 573–586.
14. Lein ES, Hawrylycz MJ, Ao N *et al.* Genome-wide atlas of gene expression in the adult mouse brain. *Nature* 2007; **445**: 168–176.
15. Lappe-Siefke C, Goebbels S, Gravel M *et al.* Disruption of Cnp1 uncouples oligodendroglial functions in axonal support and myelination. *Nat Genet* 2003; **33**: 366–374.
16. Bifulco M, Laezza C, Stingo S, Wolff J. 2′,3′-Cyclic nucleotide 3′-phosphodiesterase: a membrane-bound, microtubule-associated protein and membrane anchor for tubulin. *Proc Natl Acad Sci USA* 2002; **99**: 1807–1812.
17. Lee J, Gravel M, Zhang R, Thibault P, Braun PE. Process outgrowth in oligodendrocytes is mediated by CNP, a novel microtubule assembly myelin protein. *J Cell Biol* 2005; **170**: 661–673.
18. Hinman JD, Chen CD, Oh SY, Hollander W, Abraham CR. Age-dependent accumulation of ubiquitinated 2′, 3′-cyclic nucleotide 3′-phosphodiesterase in myelin lipid rafts. *Glia* 2008; **56**: 118–133.
19. Satoh J, Onoue H, Arima K, Yamamura T. Nogo-A and nogo receptor expression in demyelinating lesions of multiple sclerosis. *J Neuropathol Exp Neurol* 2005; **64**: 129–138.
20. Kuhlmann T, Remington L, Maruschak B, Owens T, Brück W. Nogo-A is a reliable oligodendroglial marker in adult human and mouse CNS and in demyelinated lesions. *J Neuropathol Exp Neurol* 2007; **66**: 238–246.
21. Muraro PA, Kalbus M, Afshar G, McFarland HF, Martin R. T cell response to 2′,3′-cyclic nucleotide 3′-phosphodiesterase (CNPase) in multiple sclerosis patients. *J Neuroimmunol* 2002; **130**: 233–242.
22. Onoue H, Satoh JI, Ogawa M, Tabunoki H, Yamamura T. Detection of anti-Nogo receptor autoantibody in the serum of multiple sclerosis and controls. *Acta Neurol Scand* 2007; **115**: 153–160.

SUPPORTING INFORMATION

Additional Supporting Information may be found in the online version of this article:

Table S1 The complete list of the proteins immobilized on a human protein microarray utilized in the present study
Table S2 The list of 82 NIG interactors identified by protein microarray

Please note: Wiley-Blackwell are not responsible for the content or functionality of any supporting materials supplied by the authors. Any queries (other than missing material) should be directed to the corresponding author for the article.

Cell Mol Neurobiol (2010) 30:415–426
DOI 10.1007/s10571-009-9466-3

ORIGINAL RESEARCH

Stable Expression of Neurogenin 1 Induces LGR5, a Novel Stem Cell Marker, in an Immortalized Human Neural Stem Cell Line HB1.F3

Jun-ichi Satoh · Shinya Obayashi · Hiroko Tabunoki · Taeko Wakana · Seung U. Kim

Received: 15 August 2009 / Accepted: 25 September 2009 / Published online: 8 October 2009

Abstract Neural stem cells (NSC) with self-renewal and multipotent properties serve as an ideal cell source for transplantation to treat spinal cord injury, stroke, and neurodegenerative diseases. To efficiently induce neuronal lineage cells from NSC for neuron replacement therapy, we should clarify the intrinsic genetic programs involved in a time- and place-specific regulation of human NSC differentiation. Recently, we established an immortalized human NSC clone HB1.F3 to provide an unlimited NSC source applicable to genetic manipulation for cell-based therapy. To investigate a role of neurogenin 1 (Ngn1), a proneural basic helix-loop-helix (bHLH) transcription factor, in human NSC differentiation, we established a clone derived from F3 stably overexpressing Ngn1. Genome-wide gene expression profiling identified 250 upregulated genes and 338 downregulated genes in Ngn1-overexpressing F3 cells (F3-Ngn1) versus wild-type F3 cells (F3-WT). Notably, leucine-rich repeat-containing G protein-coupled receptor 5 (LGR5), a novel stem cell marker, showed an 167-fold increase in F3-Ngn1, although transient overexpression of Ngn1 did not induce upregulation of LGR5, suggesting that LGR5 is not a direct transcriptional target of Ngn1. KeyMolnet, a bioinformatics tool for analyzing molecular relations on a comprehensive knowledgebase, suggests that the molecular network of differentially expressed genes involves the complex interaction of networks regulated by multiple transcription factors. Gene ontology (GO) terms of development and morphogenesis are enriched in upregulated genes, while those of extracellular matrix and adhesion are enriched in downregulated genes. These results suggest that stable expression of a single gene Ngn1 in F3 cells induces not simply neurogenic but multifunctional changes that potentially affect the differentiation of human NSC via a reorganization of complex gene regulatory networks.

Keywords HB1.F3 · KeyMolnet · LGR5 · Microarray · Neural stem cells · Neurogenin 1

Electronic supplementary material The online version of this article (doi:10.1007/s10571-009-9466-3) contains supplementary material, which is available to authorized users.

J. Satoh (✉) · S. Obayashi · H. Tabunoki · T. Wakana
Department of Bioinformatics and Molecular Neuropathology, Meiji Pharmaceutical University, 2-522-1 Noshio, Kiyose, Tokyo 204-8588, Japan
e-mail: satoj@my-pharm.ac.jp

S. U. Kim
Division of Neurology, Department of Medicine, University of British Columbia Hospital, University of British Columbia, Vancouver, BC, Canada

S. U. Kim
Medical Research Institute, Chung-Ang University College of Medicine, Seoul, Korea

Abbreviations

bHLH	Basic helix-loop-helix
CNS	Central nervous system
DAVID	Database for annotation visualization and integrated discovery
DEG	Differentially expressed genes
FBS	Fetal bovine serum
GAS2	Growth arrest-specific 2
GO	Gene ontology
HAS2	Hyaluronan synthase 2
LGR5	Leucine-rich repeat-containing G protein-coupled receptor 5
MMP9	Matrix metallopeptidase 9
Ngn1	Neurogenin 1